Cell

A Mechanism for Tunable Autoinhibition in the Structure of a Human Ca^{2+}/Calmodulin-Dependent Kinase II Holoenzyme

Luke H. Chao,[1,2,3,4] Margaret M. Stratton,[1,2,3,4] Il-Hyung Lee,[2,3,4] Oren S. Rosenberg,[1,2,3,4,11] Joshua Levitz,[5] Daniel J. Mandell,[6,7] Tanja Kortemme,[6,7] Jay T. Groves,[2,3,4,5,9,10] Howard Schulman,[8] and John Kuriyan[1,2,3,4,5,10,*]
[1]Department of Molecular and Cell Biology
[2]Department of Chemistry
[3]California Institute for Quantitative Biosciences (QB3)
[4]Howard Hughes Medical Institute
[5]Biophysics Graduate Group
University of California, Berkeley, CA 94720, USA
[6]California Institute for Quantitative Biosciences (QB3)
[7]Department of Bioengineering and Therapeutic Sciences
University of California San Francisco, San Francisco, CA 94143, USA
[8]Allosteros Therapeutics, Sunnyvale, CA 94089-1202, USA
[9]Materials Sciences Division
[10]Physical Biosciences Division
Lawrence Berkeley National Laboratory, Berkeley, CA 94720, USA
[11]Present address: Department of Medicine, University of California San Francisco, San Francisco, CA 94143, USA
*Correspondence: kuriyan@berkeley.edu
DOI 10.1016/j.cell.2011.07.038

SUMMARY

Calcium/calmodulin-dependent kinase II (CaMKII) forms a highly conserved dodecameric assembly that is sensitive to the frequency of calcium pulse trains. Neither the structure of the dodecameric assembly nor how it regulates CaMKII are known. We present the crystal structure of an autoinhibited full-length human CaMKII holoenzyme, revealing an unexpected compact arrangement of kinase domains docked against a central hub, with the calmodulin-binding sites completely inaccessible. We show that this compact docking is important for the autoinhibition of the kinase domains and for setting the calcium response of the holoenzyme. Comparison of CaMKII isoforms, which differ in the length of the linker between the kinase domain and the hub, demonstrates that these interactions can be strengthened or weakened by changes in linker length. This equilibrium between autoinhibited states provides a simple mechanism for tuning the calcium response without changes in either the hub or the kinase domains.

INTRODUCTION

Calcium/calmodulin-dependent kinase II (CaMKII) is unique among protein kinases because it forms a dodecameric holoenzyme that responds not just to the amplitude but also to the frequency of the activating signal. CaMKII is of central importance in neuronal signaling because it transduces intracellular calcium influx into the phosphorylation of ion channels, resulting in changes that alter synaptic strength (Kennedy et al., 1983; Nairn et al., 1985; Schulman and Greengard, 1978). The activity of CaMKII is switched on by calcium spikes, but the enzyme escapes calcium dependence when the calcium spike frequency exceeds a characteristic threshold.

Calcium/calmodulin (Ca^{2+}/CaM) activates CaMKII by displacing an inhibitory segment that blocks the active site of the enzyme. This segment is phosphorylated in a frequency-dependent manner, and once phosphorylated it no longer blocks the enzyme, even in the absence of Ca^{2+}/CaM (De Koninck and Schulman, 1998; Hanson et al., 1989; Miller and Kennedy, 1986). In this way, the enzyme is capable of storing a molecular "memory" of activating pulse trains, a property responsible for the key role played by CaMKII in the acquisition of long-term potentiation (LTP) (Malenka and Bear, 2004).

Each subunit of a CaMKII holoenzyme consists of a Ser/Thr-specific kinase domain followed by a regulatory segment that binds to Ca^{2+}/CaM (Hudmon and Schulman, 2002) (Figure 1). The regulatory segment is followed by a flexible linker of variable length that connects to the hub domain (also referred to as the association domain). The hub domains assemble into two hexameric rings that form the dodecameric holoenzyme (Hoelz et al., 2003; Rellos et al., 2010; Shen and Meyer, 1998).

Several structures of the isolated kinase domain, determined previously, illustrate how the regulatory segment controls kinase activity (Figure S6 available online). Three critical phosphorylation sites (Thr286, Thr305, and Thr306) are located within the regulatory segment, which is divided into three regions denoted

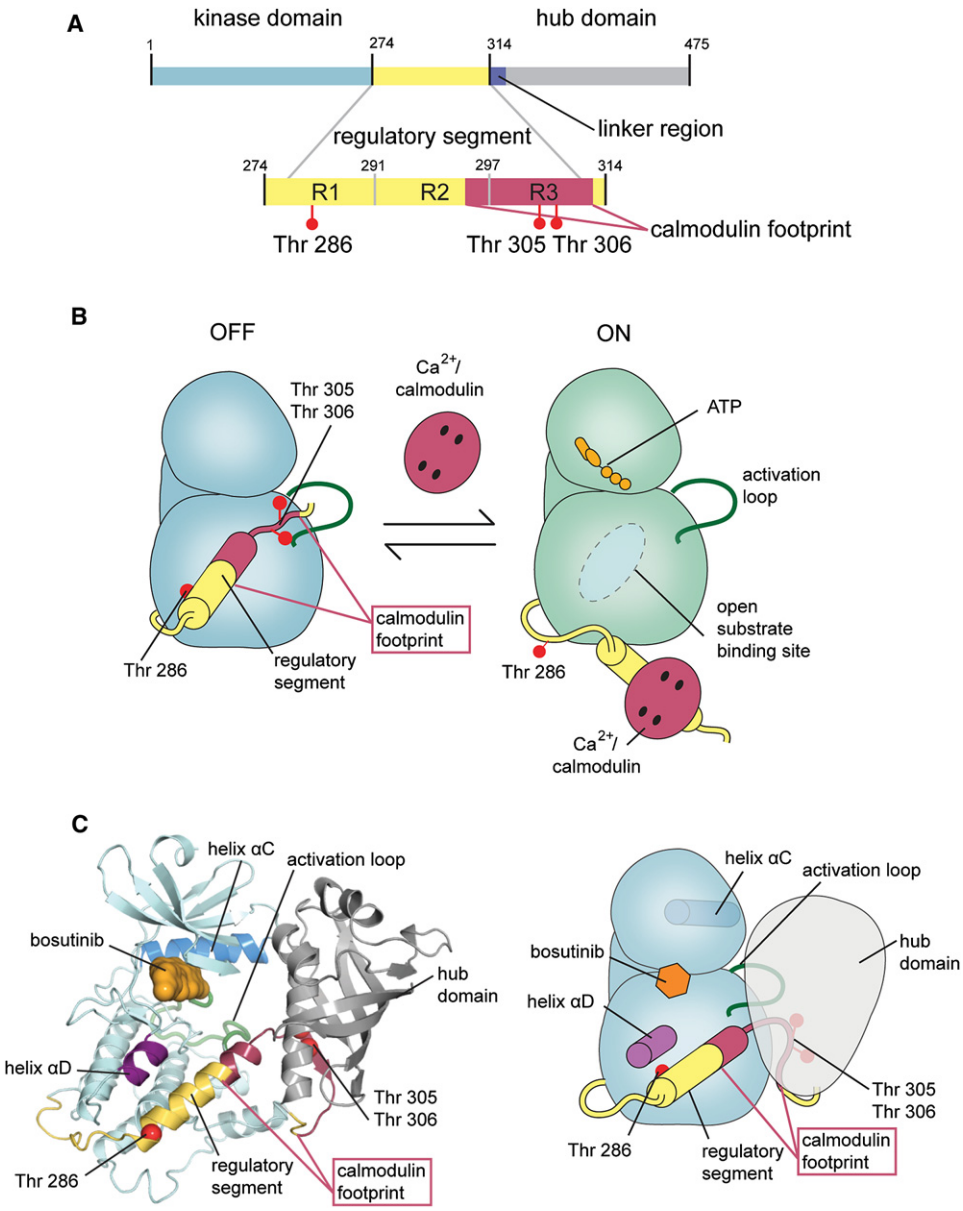

Figure 1. CaMKII Subunit Architecture and Activation

(A) Domain architecture of an individual CaMKII subunit: the kinase domain (blue) is followed by a regulatory segment (yellow and burgundy), a variable linker region (dark blue), and the hub domain (gray). The regulatory segment is comprised of the R1 element (containing the autophosphorylation site Thr286), the R2 element (an intramolecular clamp that docks the regulatory segment), and the calmodulin-binding region, R3. The calmodulin-binding footprint overlaps R3 and a portion of R2 (burgundy).

(B) Activation of subunits in the holoenzyme proceeds via regulatory segment displacement by Ca^{2+}/CaM binding to enable access and presentation of Thr286 for phosphorylation by other subunits.

(C) Structure of an individual CaMKII subunit in the crystallized holoenzyme. The regulatory segment (yellow) extends from the C terminus of the kinase domain in an α helix, then dissolves and makes a tight turn to incorporate itself into the β sheet of the hub domain.

See also Figure S1 and Figure S6.

R1, R2, and R3 (see Figure 1A). Thr286 (mouse α isoform numbering) is at the base of an α helix formed by the regulatory segment. This α helix blocks substrate binding in the autoinhibited structure by occupying a hydrophobic groove on the kinase domain. Thr305 and Thr306 lie at the heart of the calmodulin-binding region of the regulatory segment (the R3 element). Phosphorylation at Thr286 occurs in *trans*, between two kinase subunits of the same holoenzyme (Hanson et al., 1994), and disrupts the docking of the R1 and R2 elements of the regulatory segment against the kinase domain (Figure 1B). This releases autoinhibition, even in the absence of calcium, thereby conferring calcium-independent activity to the kinase. Phosphorylation

of Thr305 and Thr306 prevents calmodulin binding (Colbran, 1993; Hanson and Schulman, 1992). Studies using transgenic mice show that mutation of Thr286, a site of phosphorylation in the regulatory segment, results in impaired learning, whereas mutation of the two other phosphorylation sites (Thr305 and Thr306) results in learning that is less adaptable (Elgersma et al., 2002; Silva et al., 1992).

There are four CaMKII genes (α, β, γ, δ) in humans. The enzymes produced by these genes have virtually identical kinase domains (∼95% sequence identity) and very similar hub domains (∼80% identity). The principal difference between these gene products is in the linker connecting the kinase domain to the hub domain, which is variable in both sequence and length. At least 38 distinct mammalian splice variants are generated by lengthening or shortening this region (Tombes et al., 2003), and changes in the linker length are correlated with changes in the frequency response of the enzyme (Bayer et al., 2002). The origin of the coupling between linker length and the frequency response is unclear.

All of the essential features of CaMKII are conserved across metazoans. The regulatory segment and the three phosphorylation sites within it are invariant. The residues that mediate the oligomerization of the hub domain are conserved from representatives of the earliest metazoans, such as hydra and sea urchins, to humans (Figure S1). This conservation in CaMKII dates to the evolutionary stage when the first synapse was thought to have formed (Ryan and Grant, 2009). The linker region between the regulatory segment and hub domain is the only major site of variation over the ∼1200 million year evolution of this enzyme.

Some information about the quaternary structure of the CaMKII holoenzyme assembly has emerged from electron microscopy (EM) and small-angle X-ray scattering (SAXS). In one set of EM reconstructions, individual kinase domains are arranged above and below the midplane of the central hub (Kolodziej et al., 2000; Woodgett et al., 1984). In another set of EM reconstructions, the kinase domains occupy radial positions at the midplane of the central hub and are in close proximity to one another (Morris and Török, 2001). The radial arrangement of kinase domains in this set of EM reconstructions is similar to that seen in models of CaMKII based on SAXS (Rosenberg et al., 2005). These disparate views of the holoenzyme structure have not been reconciled.

We now present the crystal structure of the full-length dodecameric human isoform of CaMKII in an autoinhibited state. This structure reveals an unanticipated and very compact arrangement of kinase domains around the central hub. A portion of the regulatory segment, bearing the phosphorylation sites Thr305 and Thr306, is incorporated into the tertiary structure of the subunits of the central hub. We present SAXS and biochemical data indicating that the compact conformation of the holoenzyme seen in the crystal is present in solution and that the equilibrium between compact and extended forms is altered by changing the length of the linker. Analysis of a stochastic kinetics computational model for CaMKII shows that alterations in the equilibrium constant between the compact and extended forms of the holoenzyme can alter the frequency response of the enzyme. Based on these observations, we propose that a dynamic equilibrium between compact and extended autoinhibited states modulates CaMKII autoinhibition to set a tunable threshold for the response to calcium spikes.

RESULTS AND DISCUSSION

Crystallography and Structure Determination

We determined the crystal structure of an essentially full-length variant of the human CaMKII holoenzyme (residues 7–444, with the first six residues deleted) at a resolution of 4.0/3.6 Å (see Table S1). Crystallization utilized the kinase inhibitor bosutinib, previously shown to bind to CaMKII (Puttini et al., 2006; Rix et al., 2010). The β7 isoform lacks an extended linker, which in other isoforms can be as long as 50 residues (the α isoform with the β7 linker crystallized will be referred to here as the "short-linker" construct) (Wang et al., 2000). We inactivated the kinase domain by mutation (K42M, D135N) and replaced one phosphorylation site (Thr306) by valine.

The crystals contain one CaMKII subunit in the asymmetric unit, with the dodecameric holoenzyme generated by the 622 symmetry of the crystal lattice (Figure 2). These crystals diffracted X-rays anisotropically, with strong data extending to 4.0 Å in all directions and with weak data to 3.6 Å in the a* and b* directions. The X-ray data beyond 4 Å are very weak, but inclusion of these data resulted in noticeable improvement in electron density maps (Figure S2D), so these data were retained. Despite limitations in the resolution of the X-ray data, the structure of the holoenzyme assembly could be determined reliably because high-resolution structures are available for the individual kinase and hub domains (Chao et al., 2010; Hoelz et al., 2003; Rellos et al., 2010; Rosenberg et al., 2005). The holoenzyme structure (Figure 2) was determined by molecular replacement using search models based on the C-terminal lobes of the kinase domain and the hub domain (PDB codes: 2VN9 human δ isoform and 2UX0 human γ isoform, respectively). The initial solution yielded electron density maps with clear density for the N-terminal lobe of the kinase domain, which was positioned manually. The current model has been refined to an R value of 27.3% and a free R value of 32.7% (Table S1). The analysis presented in this paper is restricted to features that are resolved unambiguously in the electron density maps.

An important and unanticipated aspect of the structure is the incorporation of a portion of the regulatory segment (residues 304–308, including the autophosphorylation sites Thr305 and Thr306) as an additional strand into the central β sheet of the hub domain (Figure 3). This β strand was clearly visible in the initial electron density maps, and the structure of this strand could be modeled unambiguously (Figure S2B). Electron density for the loops that connect this strand to the rest of the regulatory segment was not well resolved initially, so we utilized the kinematic loop closure method (Mandell et al., 2009) to generate models for these regions (residues 299–304 and residues 309–314) of the regulatory segment (see Experimental Procedures). The precise structure of these loops does not enter into the analysis presented here.

Architecture of the Holoenzyme

The two stacked hexameric rings of hub domains form the core of the holoenzyme assembly and are arranged essentially as

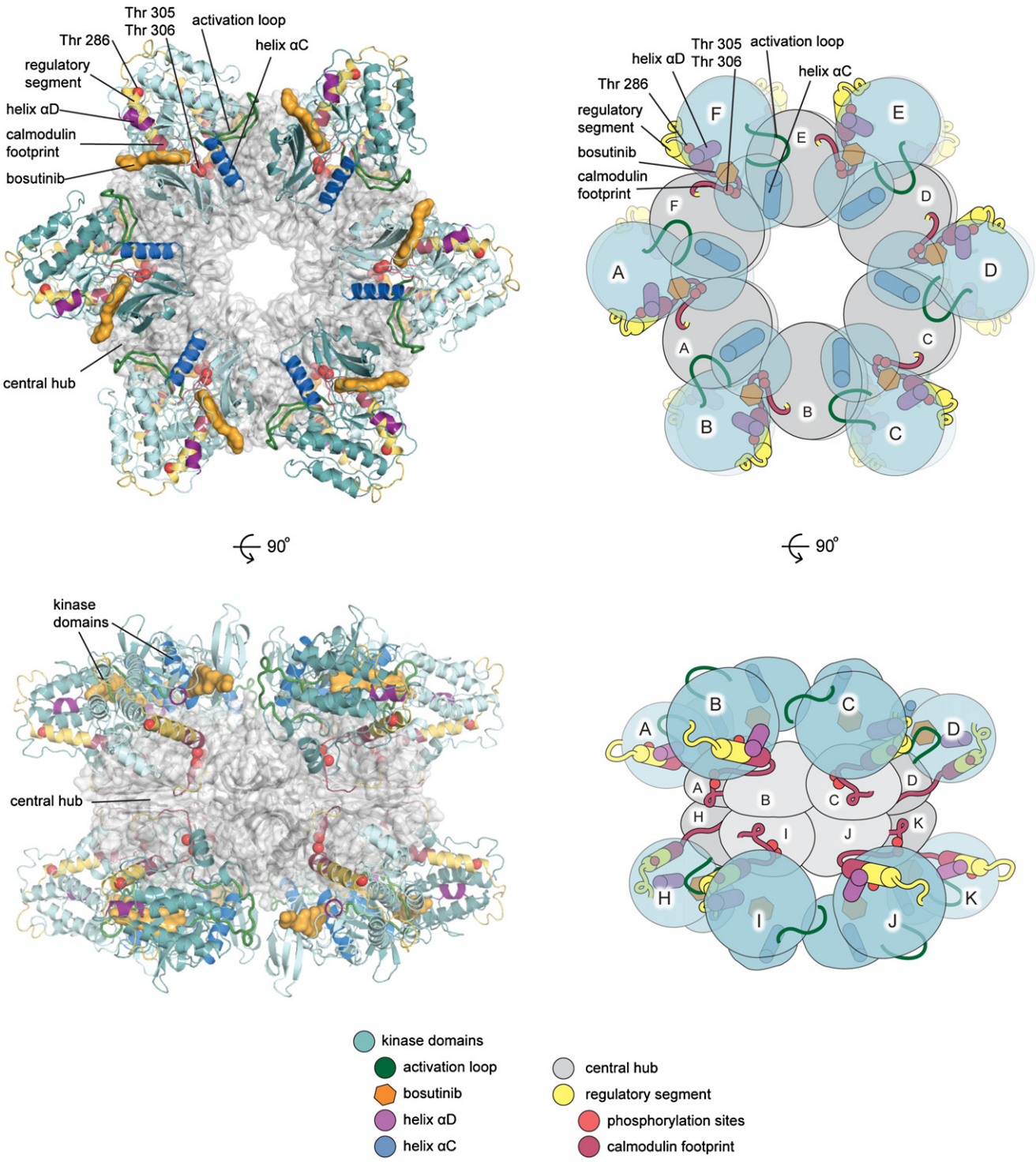

Figure 2. Domain Architecture of the Dodecameric CaMKII Holoenzyme

The holoenzyme assembly comprises kinase domains tightly arranged about the central hub domain. Each kinase domain occupies a position between two hub domain subunits, with its active site pointed toward the center of the assembly. The arrangement forms two separate hexameric rings of kinase "petals" that fold against the central hub. See also Figure S2 and Figure S3.

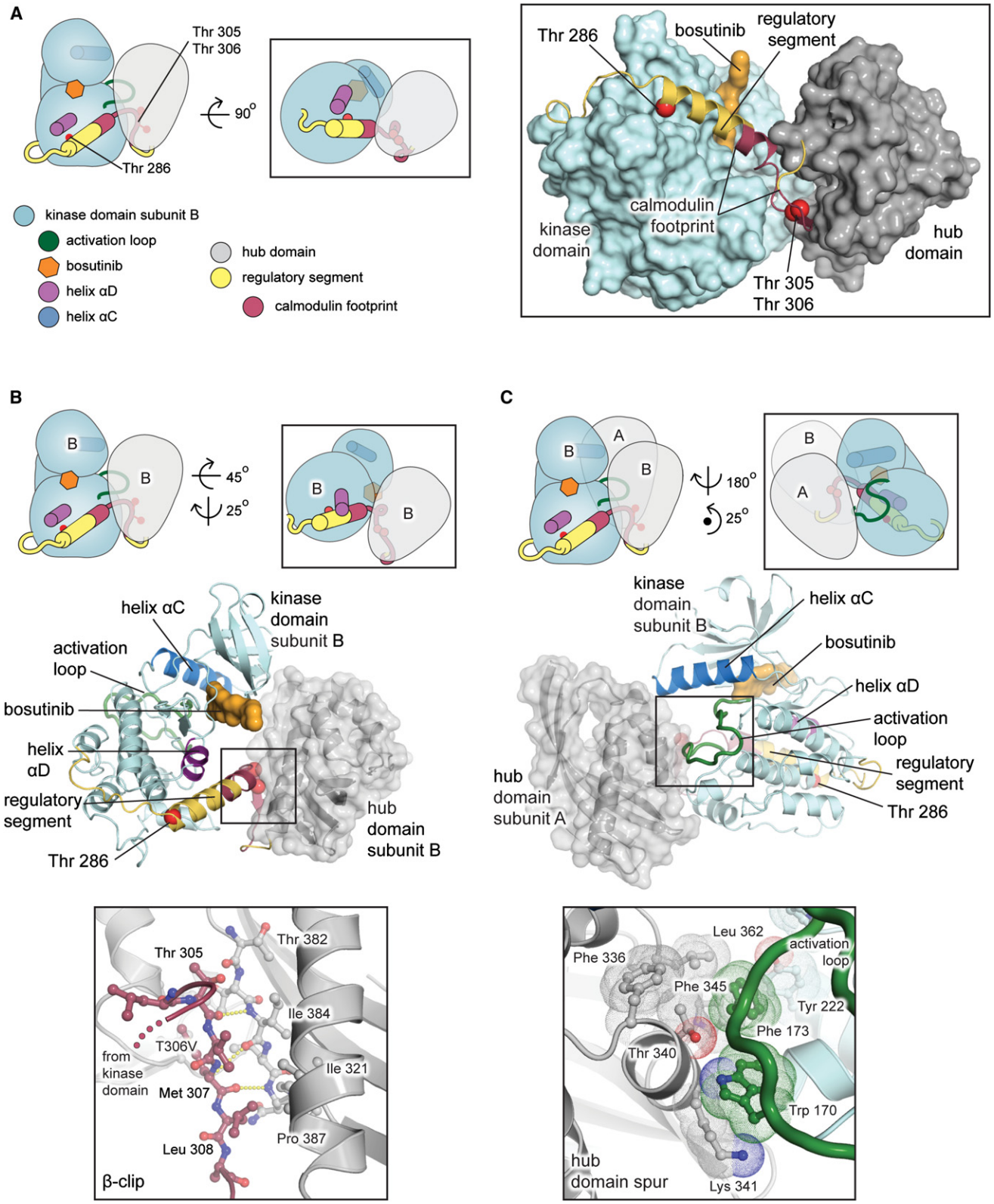
A
Thr 305
Thr 306
Thr 286
90°
kinase domain subunit B
activation loop
bosutinib
helix αD
helix αC
hub domain
regulatory segment
calmodulin footprint
Thr 286
bosutinib
regulatory segment
calmodulin footprint
kinase domain
hub domain
Thr 305
Thr 306
B
B
B
45°
25°
B
B
helix αC
kinase domain subunit B
activation loop
bosutinib
helix αD
regulatory segment
Thr 286
hub domain subunit B
C
B
A
B
180°
25°
B
A
kinase domain subunit B
helix αC
bosutinib
helix αD
activation loop
regulatory segment
Thr 286
hub domain subunit A
Thr 305
Thr 382
Ile 384
T306V
from kinase domain
Met 307
Ile 321
Pro 387
Leu 308
β-clip
Leu 362
activation loop
Phe 336
Phe 345
Tyr 222
Phe 173
Thr 340
Trp 170
hub domain spur
Lys 341

described previously (Hoelz et al., 2003; Rellos et al., 2010). Each kinase domain is positioned between two subunits of the central hub, one of which is the hub subunit to which it is connected covalently. The connections are shown in Figure 2, in which the subunits in the upper ring are named A through F in a counterclockwise sense. The kinase domain of subunit B interacts with the hub domains of subunits A and B, and so on around the ring. This arrangement creates two sets of six kinase domain "petals," one above the hub and one below, that fold against the central hub.

The quaternary assembly of the holoenzyme seen in the crystal structure has some similarity to the EM reconstructions that have kinase domains arranged above and below the midplane of the central hub (Kolodziej et al., 2000). These EM reconstructions have the kinase domains at extended positions, far from each other and from the central hub (these holoenzyme reconstructions have a roughly cylindrical shape of ~200 Å height and 140 Å diameter). In contrast, the kinase domains in the crystal structure pack tightly against the central hub (the assembly in the crystals has a cylindrical height of ~100 Å and a diameter of ~150 Å).

The R3 element of the regulatory segment connects to the hub domain. Although the R3 element is sandwiched between the kinase domain and the hub domain, the point of linkage to the hub domain occurs at the surface of the holoenzyme. This means that the extra residues present in CaMKII isoforms with longer linkers can be readily accommodated without disturbing the architecture of the holoenzyme (Figure S3C). This arrangement projects the linker regions from a central midplane of the holoenzyme, spacing linker extensions 24 and 33 Å apart to create an accessible multivalent interaction surface for binding partners.

Structure of an Autoinhibited CaMKII Subunit

Each subunit of the CaMKII holoenzyme in the crystal structure comprises a bosutinib-bound kinase domain to which the hub domain is docked tightly (Figure 1C). The conformation of the kinase domain is very similar to that seen previously for the autoinhibited form of the human δ isoform (Rellos et al., 2010), and the interaction with the hub domain appears to involve very little induced fit on the part of the kinase domain. The hub domain is arranged so that it sandwiches the regulatory segment between it and the C lobe of the kinase domain, and it makes extensive contacts with the N lobe of the kinase domain. In the standard view of the kinase domain (Figure 1C), the hub domain is located somewhat in front of the kinase domain. An adjacent hub domain from another subunit in the holoenzyme is positioned behind the first one, such that each kinase domain interacts with two hub domains (Figure 3). The two hub domains together bury ~2400 $Å^2$ of surface area at the interfaces with the kinase domain, with the contributions from the *cis*- and *trans*-interactions being ~900 and 1500 $Å^2$, respectively.

The formation of the *cis*-interface between the kinase domain and the hub domain makes the entire calmodulin recognition element inaccessible to calmodulin (Figure 3A). The R1 element of the regulatory segment exits the base of the kinase domain and continues into the R2 element to form an α helix (residues 284–300). As in other CaMKII structures, this helix abuts helix αD and locks the kinase in an inactive conformation (Figure S6). In the holoenzyme, unlike in structures of the isolated kinase domains, the R3 element is partially unfolded and makes a tight turn to interact with the hub domain.

Residues 304–308 of the R3 element form a β strand that is incorporated into the highly twisted β sheet within the core of the hub domain (Figure 3B). We refer to this interaction between the R3 element of the regulatory segment and the hub domain as the β clip. The β clip utilizes several hydrophobic residues that are strictly conserved across metazoans (Figure S1). Most notably, Thr306 (mutated to Val in the crystallization construct) lies at the heart of the β clip and interacts with Ile321, Ile384, Leu385, and Pro387 to pull the kinase domain tight against the hub domain. The presence of Thr306 at the core of the β clip predicts that phosphorylation of Thr305 and Thr306 would be incompatible with this autoinhibited form of the holoenzyme. Thr305 and Thr306 are within the calmodulin recognition element, and phosphorylation of these residues is known to prevent calmodulin rebinding (Colbran, 1993; Hanson and Schulman, 1992). Our structure now indicates that phosphorylation of these sites will also prevent adoption of the closed form of the holoenzyme in the absence of Ca^{2+}/CaM.

Kinase Domain-Central Hub Docking Interactions

An unanticipated aspect of the holoenzyme structure are the extensive interactions between the kinase domains and the central hub (Figure 3). In addition to the incorporation of the R3 portion of the regulatory segment into the hub domain, there are interactions between the kinase domain and a "spur" on an adjacent hub domain (Figure 3C and Figure 2). The hub domain spur docks against the activation loop of the adjacent kinase domain, thereby blocking access to the substrate-binding site. This interaction is analogous to the interaction between the catalytic domain of protein kinase A and its regulatory domain (Kim et al., 2007) (Figure S3).

The importance of the *trans*-interaction for CaMKII regulation is supported by the fact that residues comprising the hub domain spur interface are conserved from hydra to man. A sensitization

Figure 3. Autoinhibitory Interactions

(A) The calmodulin recognition elements are completely sequestered in each autoinhibited CaMKII subunit of the holoenzyme. Schematic of an individual kinase subunit with kinase and hub domains. Right, a zoomed-in surface representation of a subunit with the regulatory segment (yellow and burgundy) embraced by interactions from the kinase and association domains (cyan and gray, respectively).

(B) The β clip interaction. The central portion of the regulatory segment recognized by calmodulin is incorporated into the hub domain β sheet as a parallel β strand. Thr306 (mutated to valine in the crystallization construct) interacts with a hydrophobic pocket in the hub domain.

(C) The hub domain spur. The docking interaction between the kinase domain and the adjacent hub domain subunit is mediated by residues at the base of the activation loop (green) and at a spur in the hub domain.

See also Figure S3.

screen in *C. elegans* for mutants that suppress seizures identified activating mutations in CaMKII at the base of the activation loop (LeBoeuf et al., 2007). One of these mutations (G172E) maps to the center of the hydrophobic interactions at the hub domain spur interface and would be predicted to destabilize the packing of kinase domains in the autoinhibited holoenzyme arrangement that we observe (Figure S3).

Mutation of Residues at the Kinase-Hub Interfaces Alters the Activation of Human Short-Linker CaMKII

The human short-linker CaMKII construct is activated cooperatively by Ca^{2+}/CaM (Hill coefficient, n_H of 2.1) with an EC_{50} (concentration at half-maximal velocity) value of 6.0 μM (Figure 4A). This EC_{50} value for the human short-linker construct is much higher than that for isoforms with longer linkers (typically around ~25 nM), consistent with a strengthening of autoinhibition due to shortening of the linker. When the β clip region in the hub domain is mutated in the human short-linker constructs (I321E), the EC_{50} value is shifted to ~30 nM (Figure 4A). We find similar effects with mutations in the hub domain spur (Figure S4A). In addition, we also observe an elimination of cooperative activation in these mutants, with n_H ~1.0.

We investigated whether the docking interactions observed in the crystal structure influence the frequency-dependent autophosphorylation at Thr286. Utilizing a modified version of the device developed for the first in vitro studies of the CaMKII frequency response (De Koninck and Schulman, 1998), we monitored the frequency-dependent acquisition of Ca^{2+} independence ("autonomy," see Experimental Procedures). Ca^{2+}/CaM-independent autonomous activity reflects Thr286 phosphorylation and is reported as a percentage of calcium-dependent activity. We measured the acquisition of Ca^{2+}-independent activity of a human "long-linker" construct (a human α isoform of CaMKII with a 30 residue linker) in response to different frequencies of 100 ms pulses of 8 μM calmodulin (total exposure time of 6 s) and observed an exponential increase in Ca^{2+}-independent activity with respect to frequency, as shown previously (Figure 4B) (De Koninck and Schulman, 1998).

It has been observed that linker length alters the extent of Ca^{2+}-independent activity that is generated at a particular frequency (Bayer et al., 2002). We measured the Ca^{2+}-independent activity of the human short-linker construct and the human short-linker construct with a central hub mutation (I321E) under the basal conditions described above and observed no acquisition of Ca^{2+}-independent activity for either construct. We investigated the activation rates of these constructs by varying the pulse duration, from 100 ms (as mentioned above) to 350 ms. Under saturating calmodulin concentrations (12 μM), both proteins acquire Ca^{2+}-independent activity with a linear dependence on pulse duration. At low calmodulin concentrations (100 nM) there is no activation observed for the duration range tested. At intermediate calmodulin concentrations (2 and 3 μM), the short-linker mutant (I321E) displays ~2-fold higher activity compared to the short-linker construct at 350 ms pulse duration (Figure 4C). Under these conditions, the long-linker isoform acquires 100% Ca^{2+}-independent activity (data not shown). These experiments show that mutation of the interface between the kinase and the hub potentiates activation, suggesting that the kinase-hub interactions are important for autoinhibition and for setting the threshold frequency for activation.

Conformational Interconversion in the Human Short-Linker CaMKII

To address the discrepancy between the compact structure of the holoenzyme seen in our crystallographic analysis and the previously published EM and SAXS reconstructions, we measured SAXS data on several constructs of CaMKII. Solution scattering curves for the human short-linker construct and the crystallization construct (the human short-linker CaMKII with mutations K42M, D135N, and T306V and the inhibitor bosutinib) are superimposable, and the values for the radius of gyration (R_g) derived from both sets of data are 61 Å. This indicates that the structure of the holoenzyme is not altered substantially by the mutations and the addition of bosutinib (Figure S5A). We compared the experimental scattering data for this construct with theoretical scattering curves calculated from the crystal structure using the program CRYSOL (Svergun et al., 1995) (Figure S5A). The R_g value calculated from the crystal structure (55 Å) is smaller than that derived from the SAXS data (61 Å) and may reflect interconversion in solution between fully closed and more open forms.

Ab initio shape reconstructions based on the experimental SAXS data produce shape envelopes that recapitulate the diameter (~150 Å) and height (~100 Å) of the crystal structure (Figure 4D). Superposition of the crystal structure on the SAXS envelope shows that the shape reconstruction only partially accounts for the kinase domain positions above and below the central midplane. Nevertheless, the dimensions of the ab initio reconstructions are significantly smaller than the previous SAXS and EM models for long-linker constructs (which have at least one dimension of ~200 Å). The fact that the ab initio reconstructions match the dimensions of the crystal structure indicates that the compact state observed in the crystal is represented in the solution SAXS scattering data.

We measured SAXS data for short-linker holoenzyme constructs that were mutated individually at the two conserved docking sites in the hub domain: the β clip region (I321E) and hub domain spur (T340E, L362E). When mutations are made in the hub domain portion of the interface, the solution scattering data demonstrate notable increases in the value of R_g (from 61 Å to 66 Å) and changes in the scattering curve (Figure S5B). The ab initio reconstructions produce a dramatically different disc-like shape for these variants that is distinct from the more compact reconstruction obtained from human short-linker CaMKII (Figure 4D).

Linker Length Determines whether the Holoenzyme Occupies a Compact or Extended Autoinhibited Conformation

The extended disc-like SAXS reconstructions obtained for the human short-linker constructs with mutations in the central hub bear striking similarity to SAXS reconstructions obtained for the *C. elegans* CaMKII holoenzyme (Figure 5A) (Rosenberg et al., 2005). The key difference between the *C. elegans* CaMKII and the human short-linker construct is that the linker is ~30 residues longer in the *C. elegans* construct (Figure S1). We collected

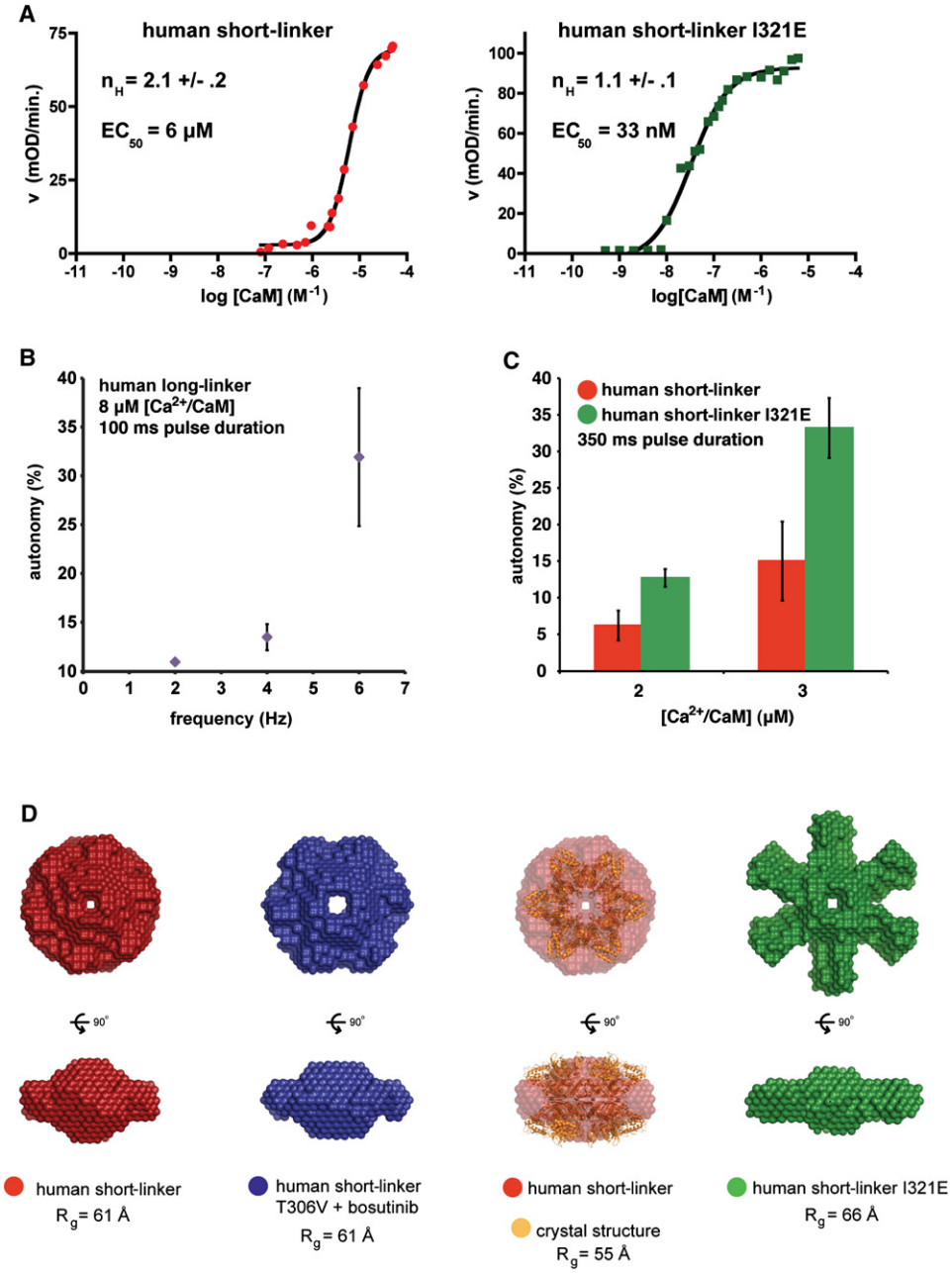

Figure 4. Human Short-Linker CaMKII Activation and Conformation

(A) Central hub mutation results in a decreased EC_{50} and a reduced n_H. The human short-linker CaMKII shows high cooperativity and a μM EC_{50} value, whereas a human short-linker CaMKII with central hub mutation shows noncooperative activation and a nM EC_{50} value. Error bars and ± terms expressed are standard error of the mean (SEM).

(B) Autonomous activity of the long-linker CaMKII increases with the frequency of stimuli (100 ms pulse durations). Error bars and ± terms expressed are SEM.

(C) Short-linker human CaMKII autonomous activity (red) compared with autonomous activity of short-linker CaMKII with a mutation at the β clip docking interaction (green) (350 ms pulse duration, at 2 and 3 μM CaM). Error bars and ± terms expressed are SEM.

(D) SAXS shows conversion from a compact to an extended state upon central hub mutation (green). Shape reconstructions are unchanged upon T306V mutation and addition of bosutinib (blue) and match the dimensions of the crystallized holoenzyme (transparent red envelope) when compared to the crystal structure (orange).

See also Figure S4 and Figure S5.

SAXS data on a sample of *C. elegans* CaMKII with its linker segment deleted and observed scattering curves corresponding to a reduced R_g value (61 Å) and ab inito shape reconstructions that resemble those for the human short-linker CaMKII. Likewise, when we measure data from human long-linker CaMKII (the α isoform, which has an ~30 residue linker), we obtain scattering

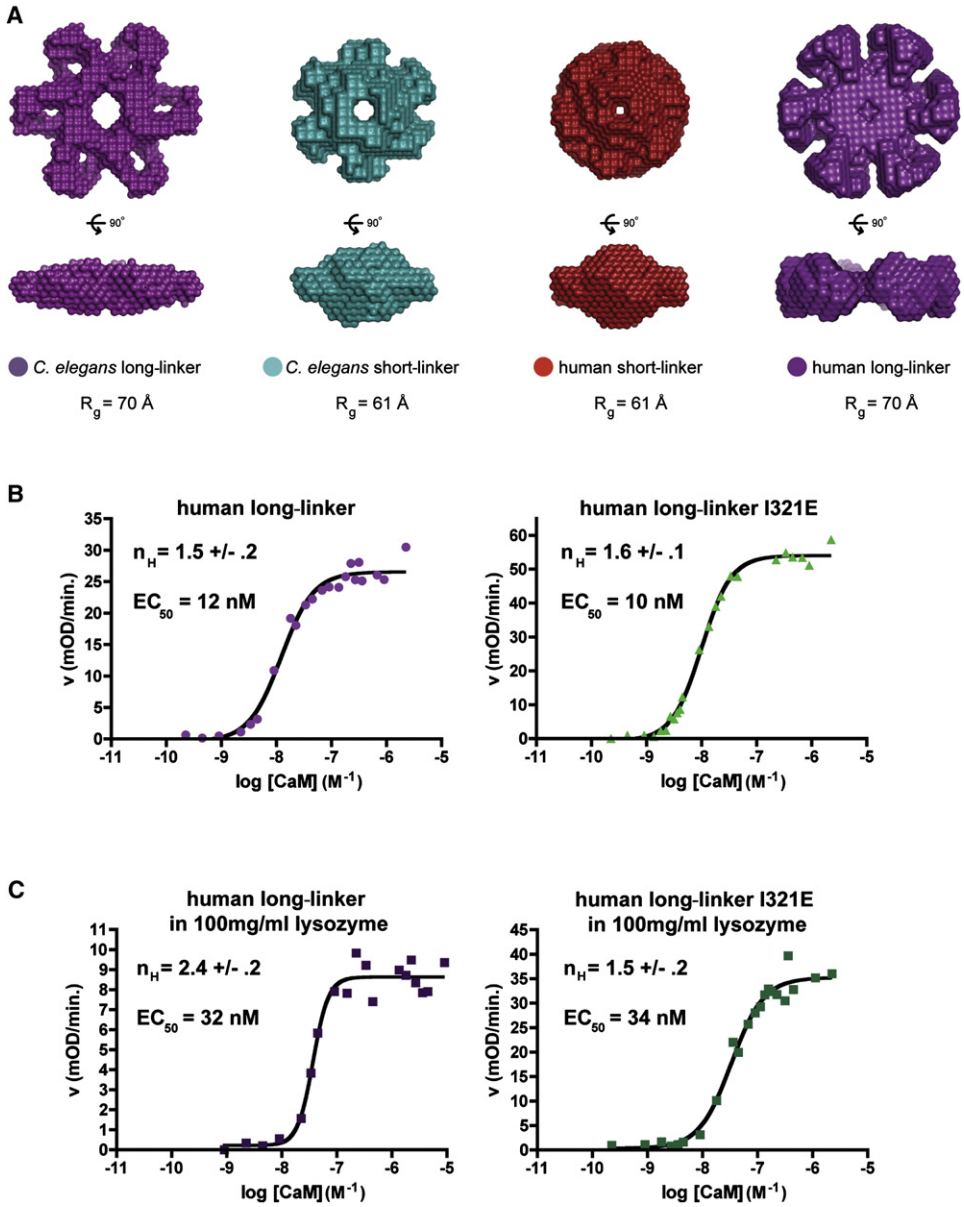

Figure 5. Long-Linker CaMKII Conformation and Activity

(A) SAXS shows conversion between an extended and compact state. *C. elegans* CaMKII has a long linker and displays an extended SAXS reconstruction (purple, left). Deletion of this linker results in a compact shape reconstruction (cyan) similar to that observed for human short-linker constructs (red). Human long-linker CaMKII also shows an extended state (purple, right). Previous SAXS and FRET analyses indicate that Ca^{2+}/CaM binding further unravels the complex to an even more extended form (Rosenberg et al., 2005; Thaler et al., 2009).

(B) Human long-linker CaMKII activates cooperatively with a nM EC_{50} value, and these properties are unaffected by mutation of the central hub. Error bars and ± terms expressed are SEM.

(C) Ca^{2+}/CaM-dependent activation of human long-linker CaMKII shows increased cooperativity when measured under conditions of molecular crowding, which is lost upon mutation of the docking interactions. Error bars and ± terms expressed are SEM.

See also Figure S4 and Figure S5.

curves and extended shape reconstructions similar to those obtained for the *C. elegans* CaMKII and the mutated human short-linker form. The SAXS data for the *C. elegans* CaMKII have been interpreted previously in terms of dimers of CaMKII kinase domains arranged around the central hub, but direct evidence for this model is lacking (Rosenberg et al., 2005). Previous SAXS and FRET analyses indicate that the extended autoinhibited assembly unravels further to an even more extended form upon Ca^{2+}/CaM binding (Rosenberg et al., 2005; Thaler et al., 2009).

These data suggest that the length of the linker determines the distribution of conformations of the holoenzyme in solution, and that changes in the linker length alter the equilibrium between the compact form observed in the crystal structure and a more extended disc-like form. The ability to interconvert between compact and extended autoinhibited conformations of both human and *C. elegans* forms of the enzymes suggests that this equilibrium is a general feature of the enzyme.

The Docking of Kinase Domains onto the Central Hub Is Also Relevant for CaMKII Isoforms with Long Linkers

Considering the high conservation of the kinase and hub domains, we reasoned that the compact holoenzyme assembly may also be relevant for isoforms with longer linkers. We measured the Ca^{2+}/CaM-dependent activation of human long-linker CaMKII and observe a level of cooperativity similar to that observed previously (Chao et al., 2010). When residues important for kinase domain-central hub docking are mutated, the Hill coefficient and the EC_{50} value for activation are unaffected (Figure 5B).

The SAXS measurements and the activity assays described previously were carried out under standard laboratory assay conditions, where protein concentrations are much lower than those found in the interior of the cell. Because the conversion between the compact and extended forms of the CaMKII holoenzyme involves a particularly large change in molecular dimensions, we expect that this conformational change would be sensitive to the density of macromolecules around the holoenzyme. In crowded cellular environments, the total concentration of protein ranges from 300–400 mg/ml (Ellis, 2001). We measured the activation of human long-linker CaMKII under simulated conditions of macromolecular crowding by using 100 mg/ml lysozyme and observe that the Hill coefficient for this construct increases from 1.4 to 2.4. The increases in the Hill coefficient and EC_{50} value are dependent on the concentration of crowding agent (Figure 5C; Figure S4B).

When the same measurement is performed with a mutant that disrupts kinase docking against the central hub (I321E), we do not observe an increased Hill coefficient, suggesting that the increase in cooperativity is dependent on the docking interactions observed in the crystal structure.

The similar levels of cooperativity observed for the human long-linker CaMKII with and without central hub mutations suggest that the extended SAXS conformation seen in dilute solution is not dependent on the docking interactions visualized in the crystal structure. Nevertheless, the fact that the Hill coefficient and the EC_{50} value both respond to the central hub mutations under crowding conditions indicates that CaMKII holoenzymes with long linkers do sample the compact state, but less frequently. Taken together, these data indicate that the linker region modulates an equilibrium between compact and extended autoinhibited states to alter the strength of docking interactions.

Simulation of CaMKII Activation by Ca^{2+}/CaM

Several computational analyses of CaMKII have been published previously (see, for example, Chiba et al., 2008; Pepke et al., 2010) but do not take explicit account of the architecture of the holoenzyme. One conclusion from these studies is that a frequency-dependent response to Ca^{2+}/CaM does not require a multimeric holoenzyme. Sensitivity to the frequency of calcium spikes arises naturally from the association and dissociation rates for the interaction of Ca^{2+} with calmodulin, the interaction of Ca^{2+}/CaM with CaMKII, and the catalytic rate constant for the phosphorylation of Thr286 on one CaMKII subunit by another. Given these conclusions, we wondered what aspect of the frequency-dependent behavior of CaMKII might be dependent on the dodecameric holoenzyme.

One property of CaMKII that must be a consequence of its assembly is the difference in frequency response that is observed for CaMKII isoforms with linkers of different lengths (Bayer et al., 2002). The high degree of conservation in sequences of the kinase domain and the regulatory segments makes it unlikely that the kinase domains of the different isoforms differ significantly in their intrinsic catalytic rate constants or in their affinity for Ca^{2+}/CaM. And yet it is apparent that isoforms with longer linkers have a higher affinity for Ca^{2+}/CaM and acquire Ca^{2+}-independent activity at lower frequencies than do isoforms with shorter linkers (Bayer et al., 2002).

The results presented earlier suggest that the length of the linker controls the equilibrium between the compact form of the holoenzyme, in which the calmodulin-binding elements are completely sequestered, and more open forms. To see how alterations in the equilibrium between open and closed states might alter the frequency response, we set up a stochastic simulation scheme (Gillespie, 1976) for the mechanism of CaMKII activation by calmodulin (Figure 6A). The holoenzyme is represented in this scheme by 12 kinase domains arrayed around a circle, with no distinction made between the upper and lower rings seen in the crystal structure. In the completely autoinhibited state, each of the kinase domains is inaccessible to Ca^{2+}/CaM. Each kinase domain can "pop-out" of the fully closed state independently of the others, governed by kinetic rates for kinase domain popping-out and retracting, k_{pop} and k_{-pop}, respectively. The equilibrium constant is the ratio of the rates, denoted K_{pop}. Only the released kinase domain can bind to Ca^{2+}/CaM, and a released kinase domain bound to Ca^{2+}/CaM facilitates the popping-out of two adjacent subunits and their binding to Ca^{2+}/CaM. This feature was introduced because the release of the regulatory subunit from one kinase domain by Ca^{2+}/CaM allows that kinase domain to capture the regulatory segment of a nearby kinase domain (Chao et al., 2010; Hoffman et al., 2011). Once two adjacent subunits are bound to Ca^{2+}/CaM they can phosphorylate each other on Thr286, leading to Ca^{2+}-independent activity.

We simulated such a reaction scheme, using kinetic rate constants and other parameters described previously (Chiba et al., 2008), except for the introduction of the pop-out equilibrium and the ability of popped-out subunits to potentiate the release of adjacent subunits (see Extended Experimental Procedures). Calcium spike trains of varying frequency were used in the simulations, consisting of alternating 100 ms square-wave pulses of 500 μM Ca^{2+} followed by a period where the Ca^{2+} concentration was zero. The interval between Ca^{2+} pulses determined the frequency of the stimulation.

We monitored the accumulation of Thr286 phosphorylation with time in these simulations, while varying the values of k_{pop}

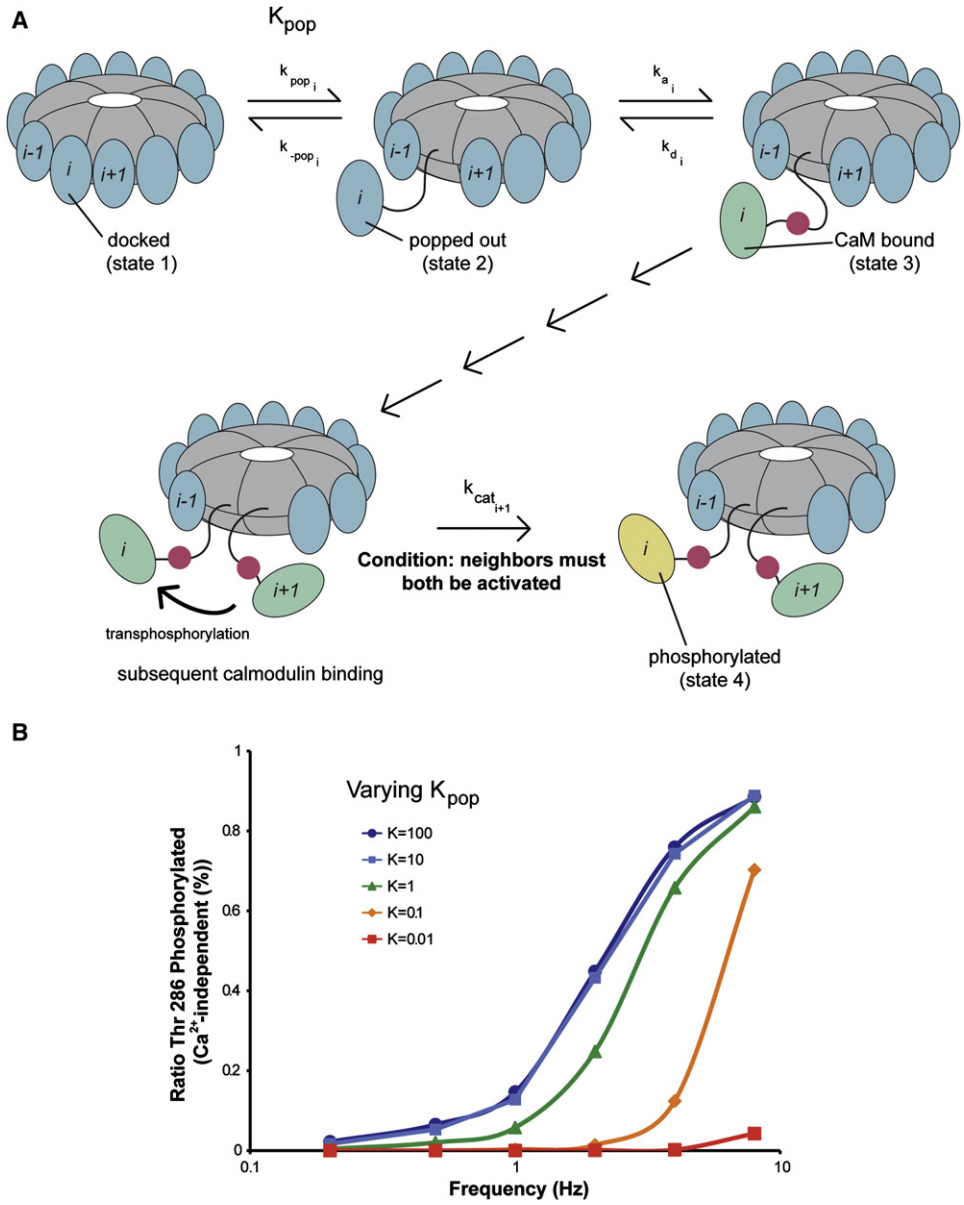

Figure 6. A Stochastic Computational Model for the CaMKII Frequency Response

(A) Scheme for simulations of CaMKII's frequency response (see Figure S7).

(B) Results for a simulation in which a popped-out subunit increases the popping-out probability of the adjacent subunit 5-fold and increases Ca^{2+}/CaM binding to the adjacent subunit 5-fold (each simulation was run for 30 s).

Data for simulations in which cooperativity was absent are shown in Figure S7C. See also Figure S7.

and k_{-pop} to change the pop-out equilibrium constant, K_{pop}, from 10^{-2} to 10^{2}. Results for a calmodulin concentration of 500 nM are shown in Figure 6B (the time evolution of different species and additional calmodulin concentrations are shown in Figure S7). These results show clearly that the stability of the closed form has a strong effect on the frequency response of the holoenzyme. When the holoenzyme is strongly biased toward the open form (K_{pop} is 10 or higher), it gains substantial Ca^{2+} independence with pulse trains between 1 and 10 Hz. In contrast, for lower values of K_{pop}, much less activity is seen for the same range of frequencies. This trend is also maintained in simulations in which a popped-out subunit does not influence the popping-out of an adjacent subunit or its ability to bind to Ca^{2+}/CaM (Figure S7C).

Our simulation results suggest that the interconversion between the open and closed forms provides an additional kinetic step in the activation of CaMKII that is readily varied without changing the catalytic machinery or the regulatory segment. Changes in the linker length might also change the rate at which kinase domains can access each other for the

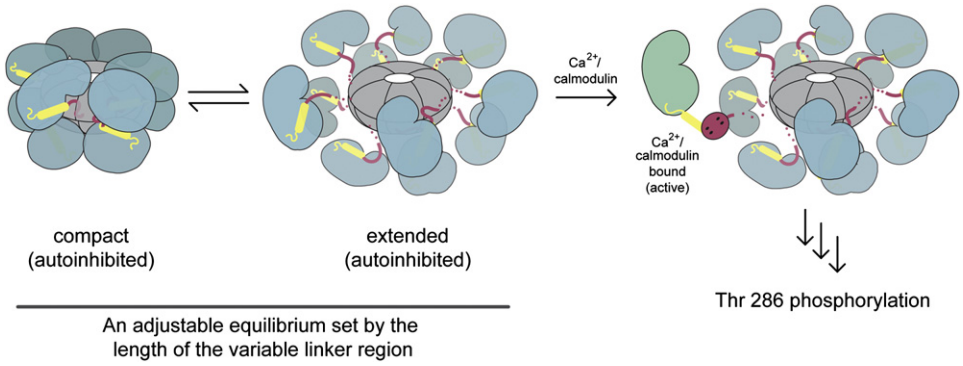

Figure 7. An Equilibrium between Compact and Open Autoinhibited States Sets the Frequency Threshold

The compact autoinhibited state is completely inaccessible to calmodulin due to docking against the central hub and incorporation of the regulatory segment into the hub domain. The compact state is in equilibrium with an extended form, where the calmodulin recognition element (shown in burgundy) is accessible. Both states are autoinhibited. Linker length alters the strength of kinase-central hub autoinhibitory interactions. Shortening the linker shifts the equilbrium toward the compact state, setting the threshold frequency to higher values. Lengthening the linker shifts the equilibrium to the extended state, setting the threshold calcium frequency to lower values.

transphosphorylation reaction, but we have not included this in our simulations because there is limited information on this aspect of the reaction.

Conclusions

We have determined the structure of the CaMKII holoenzyme in an autoinhibited state and shown how the regulation of the enzyme involves the integration of the autoinhibitory elements directly into the central hub that organizes the dodecameric assembly. The structure we have determined presumably corresponds to the most tightly inhibited assembly of the enzyme, and one in which the calmodulin-binding elements cannot be accessed by calmodulin. We have shown that CaMKII undergoes a dynamic equilibrium between this compact form and a more extended form where the kinase domains are released from the tight embrace of the central hub but are still autoinhibited (Figure 7). We surmise that it is this more extended form to which calmodulin binds, and that the response of the enzyme to the frequency of activating calcium spikes is tuned by varying the balance of this equilibrium. Our structure explains how CaMKII variants with different linker lengths are all consistent with adoption of either class of structures while having altered preferences for the set-point of the equilibrium.

A basic function of the holoenzyme architecture early in evolution may have simply been to concentrate CaMKII where it is most needed. Once the enzyme was concentrated in this way, evolutionary pressure to prevent spurious transphosphorylation would have become acute, and the holoenzyme assembly that we describe here is presumably the result. Colocalization into a homomultimeric assembly can provide evolutionary advantages for evolving allosteric control (Kuriyan and Eisenberg, 2007). The structure presented here shows that the colocalization element itself can be used as a layer of autoinhibition. Natural variants of the enzyme have essentially identical kinase and central hub domains and differ mainly in the length of the linker that controls the equilibrium between closed and open forms of the holoenzyme. This provides a mechanism whereby modulating autoinhibition tunes the calcium frequency response.

EXPERIMENTAL PROCEDURES

Protein Expression and Purification

A bacterial expression system for expression of human CaMKII was used for all protein samples and has been described previously (Chao et al., 2010). *C. elegans* constructs were prepared similarly. Full-length constructs of human CaMKII were cloned in a pSMT-3 vector containing an N-terminal Sumo tag (LifeSensors). Expression in Tuner(DE-3)pLysS cells was induced by addition of 1 mM isopropyl β-D-1-thiogalactopyranoside, grown overnight at 18°C. Cell pellets were resuspended and lysed by cell disrupter. Lysate was loaded onto a 5 ml Ni-NTA column, with buffer containing 75 mM imidazole, eluted with 1 M imidazole, and cleaved with Ulp1 protease or PreScission protease (for sumo fusion or C-terminal His-tag constructs, respectively). The final samples were buffer-exchanged by superose 6 gel-filtration chromatography (final buffer: 25 mM 1,3-bis(tris(hydroxymethyl)methylamino)propane, 150 mM potassium chloride, 2 mM dithiothreitol, 1 mM tris(2-carboxyethyl)phosphine)).

Calmodulin (from *Gallus gallus*) was expressed using a pET-15b vector (generous gift of Angus Nairn) and purified as described previously (Putkey and Waxham, 1996).

Crystallization of the CaMKII Holoenzyme

The crystallization construct comprised residues 7–444 of human α isoform of CaMKII with the β7 linker with mutations K42M, D135N, and T306V. Protein samples were concentrated in the presence of 2-fold molar excess bosutinib, which was a gift from Giulio Superti-Furga. Crystals were grown by sitting drop vapor diffusion in 1.2 M Ammonium Tartrate, 100 mM bistrispropane (pH 5.5) from repeated seeding. An additive (0.16% w/v 1,4-Diaminobutane, 0.16% w/v 1,8-Diaminooctane, 0.16% w/v Cadaverine, 0.16% w/v Cystamine dihydrochloride, 0.16% w/v Spermidine, 0.16% w/v Spermine, 0.02 M in HEPES sodium, pH 6.8) facilitated growth of crystals in a third dimension. Crystals were cryoprotected in 25% glycerol. X-ray data were collected at the Advanced Light Source beamlines 8.2.1 and 8.2.2 at 100°K, at the wavelength 0.9537 Å.

Structure Determination and Refinement

Structures were solved by molecular replacement using Phaser (McCoy et al., 2007). Refinement was performed with CNS (Brünger et al., 1998) and PHENIX (Adams et al., 2002), and model building was performed using O (Jones et al., 1991) and Coot (Emsley and Cowtan, 2004). For residue segments 299–304 and 309–314, the kinematic closure (KIC) method (Mandell et al., 2009) implemented in Rosetta revision 39011 was used to generate large numbers of potential loop models. The KIC refinement protocol was employed as described previously (Mandell et al., 2009) except for keeping the temperature fixed at k_BT = 1.2 and sampling non-pivot phi/psi torsions from a Gaussian distribution 3° above and below the value after the previous move.

Conformations of all side-chains within 10 Å of either segment were optimized after each kinematic move. Models were clustered by backbone root mean square deviation, and the best scoring models from the five largest clusters were compared against the electron density maps. The refined solution was obtained from the best scoring model from the largest cluster. All modeled residues for these regions (residues 299–304 and 309–314) were included in the final model.

Small-Angle X-Ray Scattering

SAXS data were collected at SIBYLS beamline 12.3.1 using a Mar 165 CCD area detector (165 mm diameter). Fifteen microliter samples were loaded in a 1 mm thick chamber with 25 mm mica windows by an automated robotics setup (Hura et al., 2009). Incident X-rays were tuned to a wavelength of 1.0–1.5 Å, and the detector to sample distance was 1.5 m, resulting in scattering vectors ranging from 0.007 to 0.31 $Å^{-1}$. The SAXS data were measured at three protein concentrations for each sample, with no evidence for aggregation- or concentration-dependent changes in scattering curves. The values of R_g were determined using PRIMUS (Konarev et al., 2003) and GNOM (Svergun, 1992). Eight individual shape reconstructions were generated using GASBOR (Svergun et al., 2001) and represented as average envelopes.

Enzyme Assays

Kinase activity was monitored using a continuous spectrophotometric assay (Barker et al., 1995), under conditions described previously (Chao et al., 2010). Molecular crowding measurements were performed with crowding agents added to final concentrations of 100–200 mg/ml. Reactions were initiated by the addition of 10–20 nM CaMKII to the mix, and the decrease in absorbance was monitored at 340 nm and 30°C in a microtiter plate spectrophotometer (SpectraMax). Cooperativity curves were plotted and analyzed using the program Prism (GraphPad Software) and fit to the Hill equation:

$$Y = Y_{\min} + \frac{(Y_{\max} - Y_{\min})}{1 + \left(\frac{10^{(\log_{10} EC_{50})}}{10^{(\log_{10}[L])}}\right)^{n}}$$

where Y is the maximal velocity, EC_{50} is the concentration at half -maximal velocity, [L] is the ligand concentration of calmodulin, and n is the apparent Hill coefficient, n_H.

Measurements of the threshold frequency for autonomous activation utilized a pulsed-perfusion device similar to that used previously (De Koninck and Schulman, 1998), with the radioactive assay replaced by the ADP Hunter end-point assay (DiscoverRX). CaMKII was expressed with a C-terminal biotinylation sequence (Avitag) (Howarth and Ting, 2008) and labeled using the biotin ligase BirA (efficiency accessed by mass spectrometry to be complete). CaMKII was loaded onto magnetic beads coated with streptavidin (Dynabeads MyOne, Invitrogen) and immobilized by a neodymium magnet from Gaussboys (37 mm diameter, Model C3737, pull strength 200 lbs) placed under the sample tubing (1.58 mm diameter). Following programmed pulses of Ca^{2+}/CaM (500 μM calcium, 100 nM–12 μM calmodulin, 10 mM $MgCl_2$, 250 μM ATP) and EGTA (1 mM), the protein-labeled beads were removed from the tubing, and autonomy was measured as a percentage of maximal Ca^{2+}/CaM-stimulated activity (in triplicate). Each frequency measurement consisted of a 100 ms pulse of Ca^{2+}/CaM (50 ms valve opening time) followed immediately by a pulse of 1 mM EGTA. This sequence was repeated 60 times (total activation time, 6 s) with frequency determined by the interval between pulses.

ACCESSION NUMBERS

The crystal structure has been deposited in the Protein Data Bank under ID code 3SOA.

SUPPLEMENTAL INFORMATION

Supplemental Information includes Extended Experimental Procedures, six figures, and one table and can be found with this article online at doi:10.1016/j.cell.2011.07.038.

ACKNOWLEDGMENTS

We thank Angus Nairn, André Hoelz, Sebastian Deindl, Patricia Pellicena, Paul De Koninck, Jonathan Winger, and the members of the Kuriyan Lab for many discussions and insights. We thank Giulio Superi-Furga for bosutinib, David King for peptide synthesis and mass spectrometry, Alice Ting for the BirA vector, Tony Iavarone for mass spectrometry support, and Greg Hura for SAXS data collection. We thank Tiago Barros and Joel Guenther for review of the manuscript. We acknowledge Corie Ralston and the staff at Advanced Light Source beamlines 8.2.2 and 8.2.1 for assistance with data collection. The Advanced Light Source is supported by the Director, Office of Science, Office of Basic Energy Sciences, of the U.S. Department of Energy under Contract No. DE-AC02-05CH11231.

Received: January 12, 2011
Revised: May 11, 2011
Accepted: July 29, 2011
Published: September 1, 2011

REFERENCES

Adams, P.D., Grosse-Kunstleve, R.W., Hung, L.W., Ioerger, T.R., McCoy, A.J., Moriarty, N.W., Read, R.J., Sacchettini, J.C., Sauter, N.K., and Terwilliger, T.C. (2002). PHENIX: building new software for automated crystallographic structure determination. Acta Crystallogr. D Biol. Crystallogr. *58*, 1948–1954.

Barker, S.C., Kassel, D.B., Weigl, D., Huang, X., Luther, M.A., and Knight, W.B. (1995). Characterization of pp60c-src tyrosine kinase activities using a continuous assay: autoactivation of the enzyme is an intermolecular autophosphorylation process. Biochemistry *34*, 14843–14851.

Bayer, K.U., De Koninck, P., and Schulman, H. (2002). Alternative splicing modulates the frequency-dependent response of CaMKII to Ca(2+) oscillations. EMBO J. *21*, 3590–3597.

Brünger, A.T., Adams, P.D., Clore, G.M., DeLano, W.L., Gros, P., Grosse-Kunstleve, R.W., Jiang, J.S., Kuszewski, J., Nilges, M., Pannu, N.S., et al. (1998). Crystallography & NMR system: A new software suite for macromolecular structure determination. Acta Crystallogr. D Biol. Crystallogr. *54*, 905–921.

Chao, L.H., Pellicena, P., Deindl, S., Barclay, L.A., Schulman, H., and Kuriyan, J. (2010). Intersubunit capture of regulatory segments is a component of cooperative CaMKII activation. Nat. Struct. Mol. Biol. *17*, 264–272.

Chiba, H., Schneider, N.S., Matsuoka, S., and Noma, A. (2008). A simulation study on the activation of cardiac CaMKII delta-isoform and its regulation by phosphatases. Biophys. J. *95*, 2139–2149.

Colbran, R.J. (1993). Inactivation of Ca2+/calmodulin-dependent protein kinase II by basal autophosphorylation. J. Biol. Chem. *268*, 7163–7170.

De Koninck, P., and Schulman, H. (1998). Sensitivity of CaM kinase II to the frequency of Ca2+ oscillations. Science *279*, 227–230.

Elgersma, Y., Fedorov, N.B., Ikonen, S., Choi, E.S., Elgersma, M., Carvalho, O.M., Giese, K.P., and Silva, A.J. (2002). Inhibitory autophosphorylation of CaMKII controls PSD association, plasticity, and learning. Neuron *36*, 493–505.

Ellis, R.J. (2001). Macromolecular crowding: obvious but underappreciated. Trends Biochem. Sci. *26*, 597–604.

Emsley, P., and Cowtan, K. (2004). Coot: model-building tools for molecular graphics. Acta Crystallogr. D Biol. Crystallogr. *60*, 2126–2132.

Gillespie, D.T. (1976). A general method for numerically simulating the stochastic time evolution of coupled chemical reactions. J. Comp. Physiol. *22*, 403–434.

Hanson, P.I., and Schulman, H. (1992). Inhibitory autophosphorylation of multifunctional Ca2+/calmodulin-dependent protein kinase analyzed by site-directed mutagenesis. J. Biol. Chem. *267*, 17216–17224.

Hanson, P.I., Kapiloff, M.S., Lou, L.L., Rosenfeld, M.G., and Schulman, H. (1989). Expression of a multifunctional Ca2+/calmodulin-dependent protein kinase and mutational analysis of its autoregulation. Neuron *3*, 59–70.

Hanson, P.I., Meyer, T., Stryer, L., and Schulman, H. (1994). Dual role of calmodulin in autophosphorylation of multifunctional CaM kinase may underlie decoding of calcium signals. Neuron *12*, 943–956.

Hoelz, A., Nairn, A.C., and Kuriyan, J. (2003). Crystal structure of a tetradecameric assembly of the association domain of Ca2+/calmodulin-dependent kinase II. Mol. Cell *11*, 1241–1251.

Hoffman, L., Stein, R.A., Colbran, R.J., and Mchaourab, H.S. (2011). Conformational changes underlying calcium/calmodulin-dependent protein kinase II activation. EMBO J. *30*, 1251–1262.

Howarth, M., and Ting, A.Y. (2008). Imaging proteins in live mammalian cells with biotin ligase and monovalent streptavidin. Nat. Protoc. *3*, 534–545.

Hudmon, A., and Schulman, H. (2002). Structure-function of the multifunctional Ca2+/calmodulin-dependent protein kinase II. Biochem. J. *364*, 593–611.

Hura, G.L., Menon, A.L., Hammel, M., Rambo, R.P., Poole, F.L., 2nd, Tsutakawa, S.E., Jenney, F.E., Jr., Classen, S., Frankel, K.A., Hopkins, R.C., et al. (2009). Robust, high-throughput solution structural analyses by small angle X-ray scattering (SAXS). Nat. Methods *6*, 606–612.

Jones, T.A., Zou, J.Y., Cowan, S.W., and Kjeldgaard, M. (1991). Improved methods for building protein models in electron density maps and the location of errors in these models. Acta Crystallogr. A *47*, 110–119.

Kennedy, M.B., McGuinness, T., and Greengard, P. (1983). A calcium/calmodulin-dependent protein kinase from mammalian brain that phosphorylates Synapsin I: partial purification and characterization. J. Neurosci. *3*, 818–831.

Kim, C., Cheng, C.Y., Saldanha, S.A., and Taylor, S.S. (2007). PKA-I holoenzyme structure reveals a mechanism for cAMP-dependent activation. Cell *130*, 1032–1043.

Kolodziej, S.J., Hudmon, A., Waxham, M.N., and Stoops, J.K. (2000). Three-dimensional reconstructions of calcium/calmodulin-dependent (CaM) kinase IIalpha and truncated CaM kinase IIalpha reveal a unique organization for its structural core and functional domains. J. Biol. Chem. *275*, 14354–14359.

Konarev, P.V., Volkov, V.V., Sokolova, A.V., Koch, M.H.J., and Svergun, D.I. (2003). PRIMUS - a Windows-PC based system for small-angle scattering data analysis. J. Appl. Cryst. *36*, 1277–1282.

Kuriyan, J., and Eisenberg, D. (2007). The origin of protein interactions and allostery in colocalization. Nature *450*, 983–990.

LeBoeuf, B., Gruninger, T.R., and Garcia, L.R. (2007). Food deprivation attenuates seizures through CaMKII and EAG K+ channels. PLoS Genet. *3*, 1622–1632.

Malenka, R.C., and Bear, M.F. (2004). LTP and LTD: an embarrassment of riches. Neuron *44*, 5–21.

Mandell, D.J., Coutsias, E.A., and Kortemme, T. (2009). Sub-angstrom accuracy in protein loop reconstruction by robotics-inspired conformational sampling. Nat. Methods *6*, 551–552.

McCoy, A.J., Grosse-Kunstleve, R.W., Adams, P.D., Winn, M.D., Storoni, L.C., and Read, R.J. (2007). Phaser crystallographic software. J. Appl. Cryst. *40*, 658–674.

Miller, S.G., and Kennedy, M.B. (1986). Regulation of brain type II Ca2+/calmodulin-dependent protein kinase by autophosphorylation: a Ca2+-triggered molecular switch. Cell *44*, 861–870.

Morris, E.P., and Török, K. (2001). Oligomeric structure of alpha-calmodulin-dependent protein kinase II. J. Mol. Biol. *308*, 1–8.

Nairn, A.C., Hemmings, H.C., Jr., and Greengard, P. (1985). Protein kinases in the brain. Annu. Rev. Biochem. *54*, 931–976.

Pepke, S., Kinzer-Ursem, T., Mihalas, S., and Kennedy, M.B. (2010). A dynamic model of interactions of Ca2+, calmodulin, and catalytic subunits of Ca2+/calmodulin-dependent protein kinase II. PLoS Comput. Biol. *6*, e1000675.

Putkey, J.A., and Waxham, M.N. (1996). A peptide model for calmodulin trapping by calcium/calmodulin-dependent protein kinase II. J. Biol. Chem. *271*, 29619–29623.

Puttini, M., Coluccia, A.M., Boschelli, F., Cleris, L., Marchesi, E., Donella-Deana, A., Ahmed, S., Redaelli, S., Piazza, R., Magistroni, V., et al. (2006). In vitro and in vivo activity of SKI-606, a novel Src-Abl inhibitor, against imatinib-resistant Bcr-Abl+ neoplastic cells. Cancer Res. *66*, 11314–11322.

Rellos, P., Pike, A.C., Niesen, F.H., Salah, E., Lee, W.H., von Delft, F., and Knapp, S. (2010). calmodulin complex reveals the molecular mechanism/calmodulin complex reveals the molecular mechanism of CaMKII kinase activation. PLoS Biol. *8*, e1000426.

Rix, U., Remsing Rix, L.L., Terker, A.S., Fernbach, N.V., Hantschel, O., Planyavsky, M., Breitwieser, F.P., Herrmann, H., Colinge, J., Bennett, K.L., et al. (2010). A comprehensive target selectivity survey of the BCR-ABL kinase inhibitor INNO-406 by kinase profiling and chemical proteomics in chronic myeloid leukemia cells. Leukemia *24*, 44–50.

Rosenberg, O.S., Deindl, S., Sung, R.J., Nairn, A.C., and Kuriyan, J. (2005). Structure of the autoinhibited kinase domain of CaMKII and SAXS analysis of the holoenzyme. Cell *123*, 849–860.

Ryan, T.J., and Grant, S.G. (2009). The origin and evolution of synapses. Nat. Rev. Neurosci. *10*, 701–712.

Schulman, H., and Greengard, P. (1978). Stimulation of brain membrane protein phosphorylation by calcium and an endogenous heat-stable protein. Nature *271*, 478–479.

Shen, K., and Meyer, T. (1998). In vivo and in vitro characterization of the sequence requirement for oligomer formation of Ca2+/calmodulin-dependent protein kinase IIalpha. J. Neurochem. *70*, 96–104.

Silva, A.J., Paylor, R., Wehner, J.M., and Tonegawa, S. (1992). Impaired spatial learning in alpha-calcium-calmodulin kinase II mutant mice. Science *257*, 206–211.

Svergun, D.I. (1992). Determination of the regularization parameter in indirect-transform methods using perceptual criteria. J. Appl. Cryst. *25*, 495–503.

Svergun, D.I., Barberato, C., and Koch, M.H.J. (1995). CRYSOL - a program to evaluate X-ray solution scattering of biological macromolecules from atomic coordinates. J. Appl. Cryst. *28*, 768–773.

Svergun, D.I., Petoukhov, M.V., and Koch, M.H. (2001). Determination of domain structure of proteins from X-ray solution scattering. Biophys. J. *80*, 2946–2953.

Thaler, C., Koushik, S.V., Puhl, H.L., 3rd, Blank, P.S., and Vogel, S.S. (2009). Structural rearrangement of CaMKIIalpha catalytic domains encodes activation. Proc. Natl. Acad. Sci. USA *106*, 6369–6374.

Tombes, R.M., Faison, M.O., and Turbeville, J.M. (2003). Organization and evolution of multifunctional Ca(2+)/CaM-dependent protein kinase genes. Gene *322*, 17–31.

Wang, P., Wu, Y.L., Zhou, T.H., Sun, Y., and Pei, G. (2000). Identification of alternative splicing variants of the beta subunit of human Ca(2+)/calmodulin-dependent protein kinase II with different activities. FEBS Lett. *475*, 107–110.

Woodgett, J.R., Cohen, P., Yamauchi, T., and Fujisawa, H. (1984). Comparison of calmodulin-dependent glycogen synthase kinase from skeletal muscle and calmodulin-dependent protein kinase-II from brain. FEBS Lett. *170*, 49–54.